DEVELOPMENT OF A DRY WALL CONCEPT FOR LASER IFE CHAMBERS

James P. Blanchard and Carl J. Martin
University of Wisconsin – Madison
1500 Engineering Dr.
Madison, WI 53706-1609
608-263-0391
blanchard@engr.wisc.edu

The first wall of a laser fusion chamber will experience high heat loads pulsed at 5-10 Hz with pulse widths on the order of a few microseconds. This poses a challenging problem for dry wall designs, as the wall will be susceptible to a variety of failure modes. The primary design concept of the High Average Power Laser (HAPL) project is a ferritic steel first wall coated with tungsten armor. Due to the extreme heat loads, the armor will experience high temperatures, extensive yielding, and surface cracking. In order to evaluate the ability of this design to provide a suitable lifetime, a series of experiments to simulate chamber conditions using ions, x-rays, infrared heating, and lasers is under way. These experimental efforts have been coupled with numerical modeling to help determine likely failure modes and establish design criteria for chambers. This paper compares models for the thermomechanical effects seen in the tests to those expected in a full power chamber, in order to assess the ability of the tests to mimic the actual chamber performance. The tests are found to have some limitations, but they still offer excellent approximations of the true behavior.

I. INTRODUCTION

The chamber walls in inertial fusion energy (IFE) devices will experience harsh thermal loads resulting from the deposition of energy from target implosions. The chamber design must account for these effects to ensure adequate wall life. Early wall design efforts will require detailed thermomechanical analyses including all thermal loads, nonlinear material effects, and, in some cases, phase changes due to melting or vaporization.

One design approach is to use dry walls, as has been adopted by the High Average Power Laser (HAPL)[1] program. The primary concept for the HAPL chamber wall is a tungsten-coated ferritic steel wall as illustrated in Figure 1. The heat loads in the HAPL system are delivered to the wall in the form of x-rays, neutrons, and ions, and the majority of their energy is deposited in the first few microns of the wall[2]. In some cases, a gas (xenon) is placed in the chamber to absorb some of this energy, effectively spreading the heat load over a longer time and reducing the peak wall temperatures. In all cases, the resulting thermal stresses are expected to be well above the yield stress of the tungsten coating, and the mechanical design will require consideration of fatigue and fracture to ensure a lifetime sufficient to provide an economical design for a commercial power plant.

In order to validate the dry wall design of the HAPL chamber wall and verify the calculations used, a series of test are being carried out. This paper presents a comparison of models for the thermostructural effects in these tests to those expected in a HAPL chamber in order to assess the ability of the tests to mimic the true chamber conditions.

II. CHAMBER HEAT LOADS

For these analyses, the thermal loads on an IFE chamber wall result from x-ray, ion, and neutron energy deposition. The power encapsulated in each species is typically on the order of 1, 29, and 70 percent, respectively, in laser IFE, depending on the target design and yield. The x-rays typically arrive at the wall first and deposit their energy within a few nanoseconds, and deposition largely occurs within the first micron of the wall. The neutrons arrive after 100-200 nanoseconds and are deposited over less than 20 nanoseconds. Since the neutrons have fairly long mean free paths, only a small fraction of their energy will be captured in the first wall. The ions arrive last, with deposition beginning after about 200 nanoseconds and continuing over a time span of approximately 3 microseconds, with deposition over a few microns. For these analyses, a 150 MJ target implosion in a 7 m radius chamber without gas is assumed. More details on the thermal loading may be found in reference 3.

III. VALIDATION EXPERIMENTS

Experiments must be used to validate the short and long term behavior of the tungsten coated steel design. There are no existing facilities that can precisely duplicate the conditions and threats expected in a laser fusion chamber, so the HAPL project has chosen to conduct five complementary experiments in parallel. Four of these experiments, using lasers, ions, and x-rays, are intended to simulate the conditions of the tungsten surface, while the fifth, using infrared (IR) heating, is intended to simulate the temperatures at the interface between the tungsten and the steel. The thermal parameters for the surface heating experiments are given in Table 1. For each of these facilities, the pulse length is significantly shorter than that of the ions in a laser IFE chamber. Hence, we must investigate the implications of these differences with respect to the ability of the experiments to mimic the failure modes of an IFE chamber.

TABLE 1: Parameters of Experiments Used to Simulate the Thermal Fluctuations in a Laser Fusion First Wall

Type	Maximum fluence per pulse (J/cm^2)	Deposition depth (μm)	Pulse width (ns)
Ion Beam	7	1-10	100
Pulsed Z-Pinch (X-Rays)	3000	1-2	6
Single Shot Z-Pinch (X-Rays)	7	1-2	30-50 (FWHM)
Laser	0.7	0	8

Infrared (IR) experiments will be used to simulate the thermostructural fields in the vicinity of the interface between the tungsten and steel. The pulse length on the IR source here is not short enough to duplicate the steep gradients at the tungsten surface, but the time-averaged power is more than adequate to simulate the bond fields and backside cooling conditions. In these experiments, the IR pulse is on the order of tens of milliseconds, with peak powers of tens of MW/m^2. The exact pulse length, dwell time, and power are chosen to duplicate the chamber conditions as closely as possible.

IV. FINITE ELEMENT MODELS

The thermostructural responses of the structures in the HAPL chamber and in the tests were modeled using a commercial finite element code (ANSYS). The surface heating and chamber models used axisymmetric elements. These models assume, through appropriate boundary conditions, laterally uniform heating and an infinite slab geometry. Stresses and strains calculated with these models were solely the product of thermal loads; i.e. no external mechanical or pressure loads were applied. For the chamber and surface heating models, the heat deposited by the various sources was modeled discretely and applied to the chamber surface over a characteristic depth. Because this heating was intense and highly localized near the tungsten surface, an extremely refined mesh was required here to accurately predict the thermal gradients. Chamber cooling is simulated simply by applying convection on the outside of the steel wall. A convection coefficient of 10 kW/m^2-C and fluid temperature of 400 C were assumed, and 400 C was used as the initial condition for the transient analyses. Because the model assumes laterally uniform heating, the sidewall is adiabatic. There is also no heat loss from the tungsten free surface. The boundary conditions and section dimensions are illustrated in figure 1. The material properties used for the analysis are provided in an appendix.

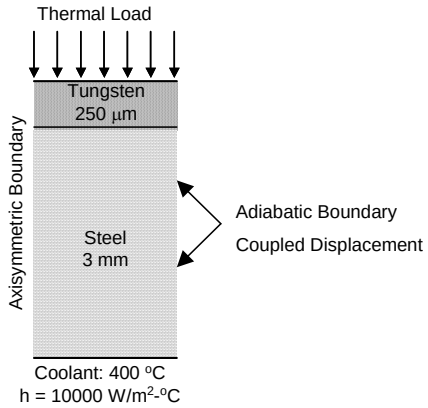

Figure 1. Wall design and FEA boundary conditions

The IR heating specimen was modeled with three-dimensional elements. Cooling channels are included in the steel wall. The cooling channels, which are more representative of potential HAPL designs, produce spatial temperature variations, and edge effects resulting from the finite specimen size can also be evaluated.

V. SURFACE RESPONSE

In this section, the transient thermostructural response near the tungsten surface will be examined for a simulated 150 MJ target implosion in a 7 m radius chamber. These results will be compared to those produced by candidate experimental loads scaled to produce identical surface temperatures. Finally, the predicted fracture stress intensities for both the chamber and experimental conditions will be compared. Further details of the chamber wall modeling can be found in reference 3.

V.A. Baseline HAPL Chamber Loading

Typical thermomechanical responses from a shot in the HAPL chamber are shown in figures 2 and 3. The transient thermal response from a single shot is illustrated in figure 2. The temperature peaks at the surface after a few microseconds. The peak temperatures will vary, depending on the target yield, chamber radius, gas pressure, etc. Figure 3 shows plastic strain histories for this same case. Clearly, significant yielding is seen on each cycle, and handling this surface deformation is one of the key challenges in designing the chamber wall.

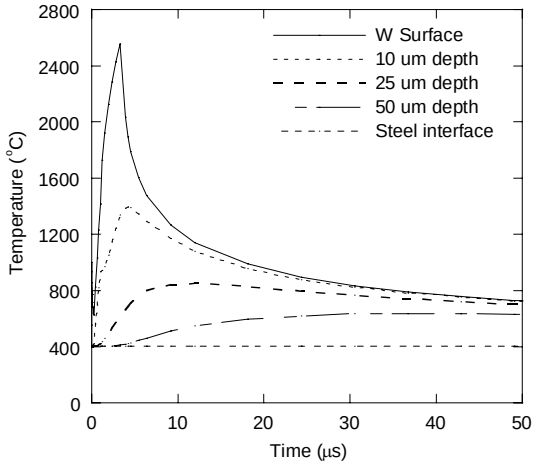

Fig. 2. Transient temperature response of the HAPL tungsten armor to the 150MJ target implosion.

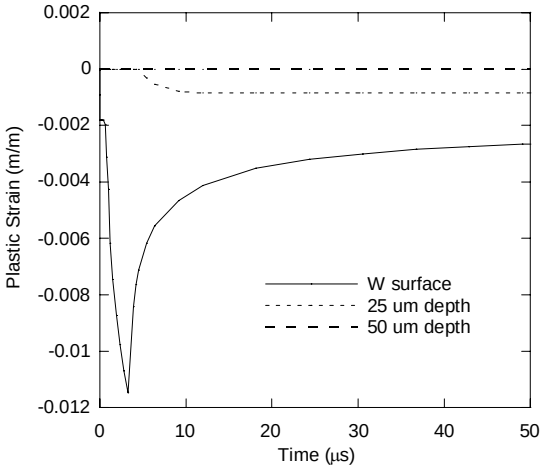

Fig. 3. Transient plastic strain near the surface of tungsten armor after 150MJ target implosion.

V.B. Validation Experiments

For each surface exposure experiment, the pulse length is significantly shorter than that of a laser IFE chamber. To compare the thermostructural fields in the experiments to that of IFE walls, we will use single pulse finite element analyses for temperature and plastic strain. These analyses, with heat fluxes adjusted to produce proper surface temperatures, are adequate for qualitative comparison, but more detailed analyses will be needed to properly use the experimental data for chamber design. The approach here is to determine the fluence necessary to duplicate the peak temperature expected from an IFE chamber pulse and compare the tungsten temperature and plastic strain for the test and chamber conditions. For comparison, the Ion Beam and Laser simulation conditions were selected with the pulse widths listed in Table 1. The temperature and plastic strain distributions near the surface of the tungsten are plotted in figures 4 and 5. The results indicate that the temperature and plastic strain at the surface can be closely simulated, but the short pulse widths of the test conditions do not allow for accurate simulation of the temperature and strain gradients into the depth. Hence while these tests are likely to be applicable for surface damage, further assessment of crack propagation into the depth of the armor is required.

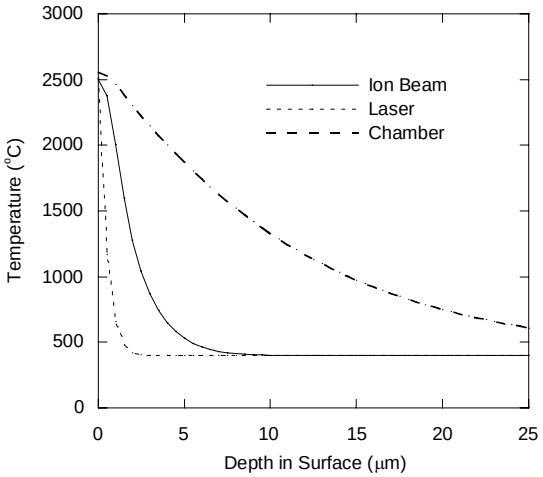

Fig. 4. Temperature distribution near the tungsten surface after heating pulse from ion beam and laser test conditions as compared with predicted chamber conditions.

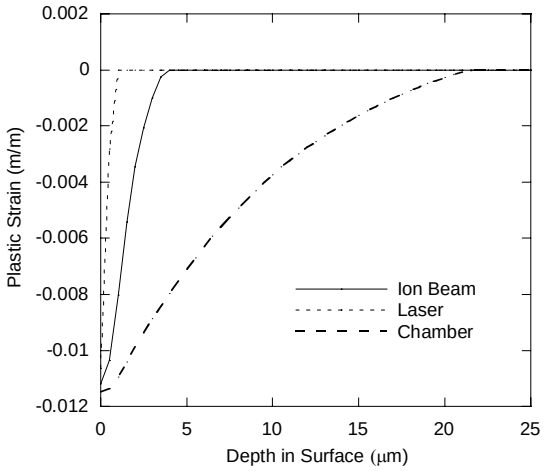

Fig. 5. Plastic strain distribution near the tungsten surface after heating pulse from ion beam and laser test conditions as compared with chamber conditions.

V.C. Fracture Analysis

Fatigue analysis under chamber conditions indicated that cyclic plasticity would induce surface cracking in the tungsten. Hence a fracture analysis was carried out to further investigate this phenomenon. These analyses,

similar to those previously described, used the singular crack tip elements and J-integral routines in ANSYS to predict the stress intensity of cracks of various depths for both the ion beam test and chamber conditions. The cracks are planar cracks along the length of the model, so they model a very long planar crack in both the HAPL chamber wall surface and in the tests. Figure 6 provides the fracture results for a HAPL wall and for the ion beam experiments. The analysis predicts that for a sufficiently thick coating the cracks are expected to arrest before reaching the steel substrate. The stress intensities predicted for the ion beam experiment are much lower, and this test will not be able to simulate the crack penetration into the substrate. However, the tests should still yield growth rate data that will be valuable for the modeling of the HAPL chamber.

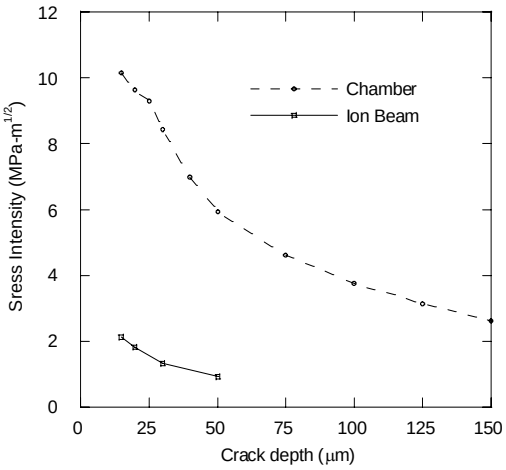

Figure 6. Variation of fracture stress intensity with crack depth in the tungsten armor. Results after a single pulse for chamber and Ion Beam test conditions.

VI. INFRARED EXPERIMENTS

IR experiments, with longer pulse lengths and lower heat fluxes, can be used to simulate the temperatures and stresses at the interface between the tungsten and steel where delamination might occur. Initially, the same convection boundary conditions and thermostructural models from the chamber analyses were used. The IR condition used (20 ms pulse width, 7.2 MW/m^2 heat flux, and 400 ms dwell time) was found to provide a good approximation of the thermal field at the coating interface. The thermal stresses seen in the infrared experiments are compared with those predicted for HAPL in Figure 7. This figure shows that these experiments can adequately duplicate the interface thermal and stress conditions of the HAPL chamber.

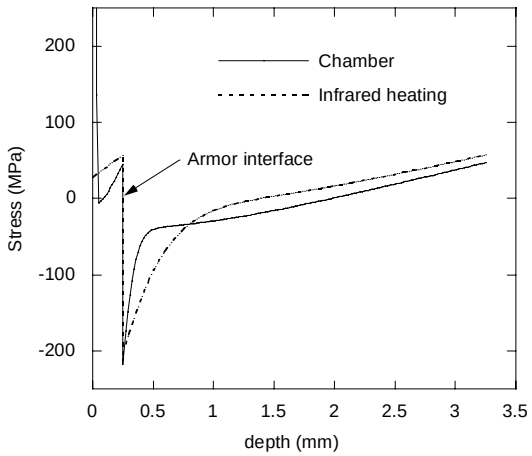

Fig. 7. Thermal stresses distribution through the armor and steel wall thickness after 50th heat pulse for HAPL base line and infrared heating simulation

VII. COOLED SAMPLES

Rather than testing generic, simple flat samples like that in Figure 1, more realistic chamber structures have been proposed for the IR experiments. One proposed IR test specimen is illustrated in Figure 8. This specimen has internal cooling channels approximating a wall design, and is relatively small with a surface area of 40 mm by 40 mm. The same convection coefficient (10 kW/m^2-C) was assumed as the chamber models, but the coolant temperature was reduced to 100 C to simplify testing. The stress distribution at the center of the specimen, as illustrated in Figure 9, compared well with those predicted previously for the flat wall model. There is a slight offset in the stress distribution that is the result of a slightly larger temperature gradient in the steel due to the limited convection area of the channels.

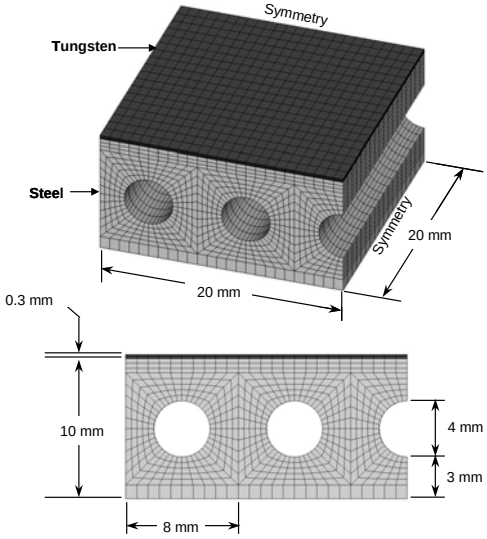

Fig. 8. Dimensions and finite element model for integral cooled IR heating specimen.

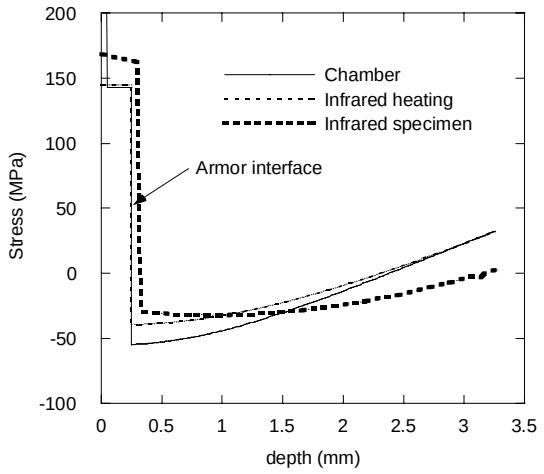

Fig. 9. Thermal stress distributions through the armor and steel wall HAPL base line, infrared heating, and cooled test specimen

Additionally, the temperature and stress variations in the panel due to the cooling channel configuration and specimen size were of interest. Temperature contours through the cross-section are illustrated in Figure 10. The variations near the surface are small with the temperatures at the interface varying by less than 0.4 C across the specimen. Variations in stress across the panel centerline are shown in Figure 11. These variations are due to both the presence of the cooling channels and edge effects. These results indicate that the 40 mm square specimen size is large enough to obtain a reasonable region of uniform stress with edge effects seen in only the outer 5 mm of the specimen.

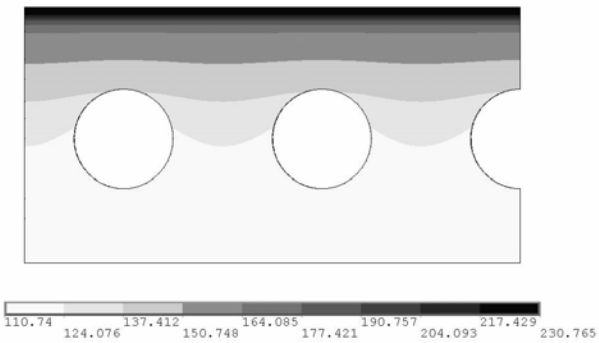

Fig. 10. Temperature contours in the cooled IR specimen at end of heating pulse.

The variation introduced by the cooling channels and the free surface are also shown in Figure 11, which displays the interface stresses parallel and perpendicular to the cooling channels. The curves exhibit a small variation in the stresses caused by the cooling channels and a larger increase at the free surface. Since the stresses in a purely elastic analysis would be singular at the intersection of the interface with the free surface, this increase in the stress is not surprising. This increase did not appear in the analysis of the flat specimens because they were modeled as infinite plates.

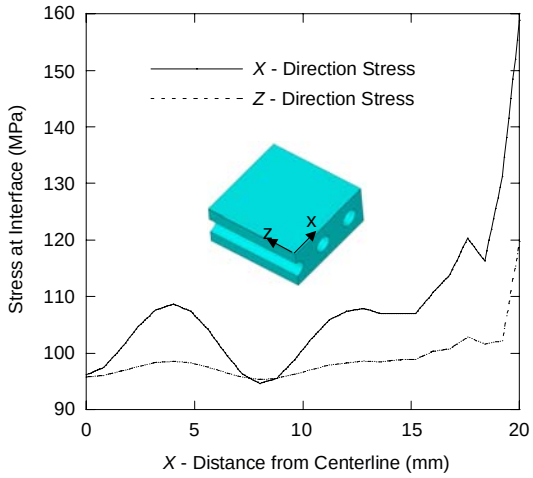

Fig. 11. Thermal stresses in the armor at the steel interface for the cooled IR test specimens

VIII. CONCLUSIONS

A tungsten-clad steel wall has been selected as the primary chamber wall design for the HAPL chamber. The tungsten surface is expected to exhibit cracking as a result of cyclic plasticity, but the cracks are expected to arrest if the tungsten coating is sufficiently thick. Tests have been devised to test these predictions, and modeling indicates that these tests will provide accurate simulations of the surface stresses and strains, but the stress intensity is lower due to the sharper surface gradient. A cooled IR specimen has been devised to further test the viability of this design and modeling indicates small variations in the stress between the coolant channels, but a large increase near the free surface.

ACKNOWLEDGEMENTS

This work was sponsored by the Naval Research Laboratory in support of the High Average Power Laser program.

REFERENCES

[1] J. Sethian, et al, “Considerations for the Chamber First Wall Material in a Laser Fusion Power Plant,” to be published in J. Nuc. Mat.
[2] R. Raffray, et al., “Chamber Threats, Design Limits And Design Windows,” to be published in J. Nuc. Mat.
[3] J. Blanchard and C. Martin, “Thermomechanical Effects in a Laser IFE First Wall,” to be published in J. Nuc. Mat.

APPENDIX – Material Properties Used in Analysis

Property	Units	Formula
TUNGSTEN		
density	[g/cm^3]	19.3027-0.00023786*T-2.2448E-8*T^2
heat capacity	[J/kg-K]	128.3+0.0328*T-3.41E-6*T^2
thermal conductivity	[W/m-K]	174.9-0.107*T+5.01E-5*T^2-7.835E-9*T^3
elastic modulus	[GPa]	398-0.00231*T-2.72E-5*T^2
Poisson's ratio		0.279+1.09E-5*T
thermal expansion coefficient	[10^{-6}K^{-1}]	3.922+5.835E-5*T+5.705E-11*T^2-2.046E-14*T^3
Tangent Modulus	[MPa]	667
Fatigue Plastic strain range	%	=34*(Nf) -0.46
STEEL		
density	[g/cm3]	7.8
heat capacity	[J/kg-K]	500+0.6*T
thermal conductivity	[W/m K]	33
elastic modulus	[GPa]	230-0.05*T
Poisson's ratio		0.29
thermal expansion coefficient	[10-6K-1]	10-0.0025*T
Tangent Modulus	[MPa]	667

Temperature (C)	Yield Stress (MPa)
TUNGSTEN	
0	1385
500	853
1000	465
1500	204
2000	57
2500	10
STEEL	
0	950
200	900
400	750
500	600
600	250
800	50